Publications of the Astronomical Society of the Pacific, 129:124204 (8pp), 2017 December https://doi.org/10.1088/1538-3873/aa8ded

TYC 1337-1137-1 and TYC 3836-0854-1: Two Low-mass Ratio, Deep Overcontact Systems Near the End Evolutionary Stage of Contact Binaries

W.-P. Liao[1,2,3], S.-B. Qian[1,2,3,4], B. Soonthornthum[5], T. Sarotsakulchai[1,4,5], L.-Y. Zhu[1,2,3,4], J. Zhang[1,2,3], and Voloshina Irina[6]
[1] Yunnan Observatories, Chinese Academy of Sciences (CAS), P.O. Box 110, 650216 Kunming, China; liaowp@ynao.ac.cn
[2] Key Laboratory for the Structure and Evolution of Celestial Objects, Chinese Academy of Sciences, 650216 Kunming, China
[3] Center for Astronomical Mega-Science, Chinese Academy of Sciences, 20A Datun Road, Chaoyang District, Beijing, 100012, China
[4] University of the Chinese Academy of Sciences, Yuquan Road 19#, Shijingshan Block, 100049 Beijing, China
[5] National Astronomical Research Institute of Thailand, 191 Siripanich Bldg., Chiang Mai 50200, Thailand
[6] Sternberg Astronomical Institute, Moscow State University, Universitetskij prospect 13, Moscow 119992, Russia; voloshina.ira@gmail.com
Received 2017 August 18; accepted 2017 September 19; published 2017 October 25

Abstract

New high-precision CCD photometric light curves of two contact binary stars, TYC 1337-1137-1 and TYC 3836-0854-1, are displayed and analyzed by using the Wilson–Devinney (W–D) program. The light curve solutions show that both of them are low-mass ratio, deep overcontact binary systems with a mass ratio of $q = 0.1716 \pm 0.0010$ and a high fillout factor of $f = 76.0 \pm 2.9\%$ for TYC 1337-1137-1, and $q = 0.1900 \pm 0.0032$ and $f = 79.4 \pm 7.9\%$ for TYC 3836-0854-1, respectively. These results indicate that they are near the end evolutionary stage of contact binaries. The absolute parameters were calculated by using the new method of mass–radius relationship ($0.238 \pm 0.009\ M_{\odot}$ and $1.386 \pm 0.050\ M_{\odot}$ for TYC 1337-1137-1, $0.228 \pm 0.014\ M_{\odot}$ and $1.20 \pm 0.07\ M_{\odot}$ for TYC 3836-0854-1, respectively). The preliminary orbital period analysis suggests that long-term period increases exist for both of them, which may be interpreted in two possible ways. A first possibility is mass transfer conservation from the less massive component to the more massive one leading to an orbital period increase. In this case, when their orbital angular momentum is less than three times the total spin angular momentum, they may evolve into a rapidly rotating single star. A second possibility is that the parabolic variation in the $(O - C)$ diagram is only a part of a long-period cyclic change caused by a potential third body. In future, more high-precision observations of these two binaries are needed to confirm the form of orbital period changes.

Key words: binaries: close – binaries: eclipsing – binaries: spectroscopic – stars: evolution – stars: individual (TYC 1337-1137-1 and TYC 3836-0854-1)

Online material: color figures, machine-readable table

1. Introduction

W UMa-type contact binaries are late-type close systems with orbital periods in the range from 0.2 to 0.5 days and effective temperatures from 4000 to 7500 K (e.g., Qian et al. 2017). Contact binary systems with mass ratios less than 0.25 and fillout factors greater than 50% are quite interesting because they are progenitors of some fascinating objects and related with several key astrophysical processes. Recent investigations showed that they may be the progenitors of luminous red novae similar to V1309 Sco (e.g., Tylenda et al. 2011; Zhu et al. 2016). They are a very important kind of binary that may further our understanding of the phenomena of blue Straggler/FK Com-type stars that is an unsolved problem (Acerbi et al. 2014). They are at the end stage of the evolution of contact binary stars and provide a good chance to study several important questions, e.g., the merger of contact binaries, mass transfer and loss. This type of low-mass ratio, deep overcontact binaries were studied by several authors (e.g., Qian et al. 2005a, 2005b, 2006, 2007, 2011; Sriram et al. 2016). In the present paper, we investigate two such systems in details.

TYC 1337-1137-1 (GSC 01337-01137, ASAS J063546 +1928.6, 2MASS J06354622+1928280) is an ASAS contact binary listed by Paczyński et al. (2006). Its period is 0.475511 days, the maximum brightness and the amplitude of variation in the V filter are $9^{\rm m}.95$ and $0^{\rm m}.43$ (Gezer & Bozkurt 2016), respectively. Thereafter, several times of light minima were published by several authors. Recently, Gezer & Bozkurt (2016) analyzed the single V band light curve with the PHOEBE software (Prša & Zwitter 2005), and preliminary photometric solutions were obtained. The absolute parameters were estimated using the correlation given by Cox (2000): $M_1 = 1.19\ M_{\odot}$, $M_2 = 0.206(5)\ M_{\odot}$, $R_1 = 1.63(1)$, and $R_2 = 0.70(1)$. They concluded that TYC 1337-1137-1 could be put into the group of low-mass ratio, deep contact binaries studied by Qian et al. (2005a). Therefore, we deemed it necessary to re-observe and re-analyze multi-color light curves

of this binary system, understand the evolutionary state, and investigate orbital period changes of TYC 1337-1137-1.

TYC 3836-0854-1 (=GSC 03836-00854, NSVS 2657878) was first identified by the Northern Sky Variability Survey (NSVS)[7] as a variable. It was initially classified as a contact binary with a period of 0.41554 days and a range of R variation between 10.134 and 10.574 magnitude by Gettel et al. (2006). The first CCD B, V and I_c symmetric light curves of TYC 3836-0854-1 were presented by Acerbi et al. (2014). They revised the orbital period to 0.4155590 days. Based on their data, TYC 3836-0854-1 was classified as a high fillout, extreme mass ratio over-contact binary (mass ratio $q = 0.206$, fillout factor $f = 59.2\%$), suggesting that it was in the late stage of over-contact evolution (Acerbi et al. 2014). The absolute parameters were estimated from the log $T_{\rm eff}$ − log L diagram: $M_1 = 1.383$ $M_\odot$, $M_2 = 0.284$ $M_\odot$, $R_1 = 1.500$, and $R_2 = 0.763$.

2. Observations and Light-curve Analysis

2.1. Observations

We observed the first CCD multi-color $BV(RI)_c$ light curves of TYC 1337-1137-1 on 2016 January 15 and 20 with the Andor 2048 × 2048 CCD photometric system connected to the 1.0 m Cassegrain reflecting telescope at Yunnan Observatories (YNOs) in China. In the observing process, the exposure times for the $BV(RI)c$ bands were set to 20 s, 10 s, 5 s, and 5 s , respectively. A total of 653, 650, 649, and 647 images in B, V, R_c , and I_c bands were obtained, respectively.

By using the 85 cm telescope at the Xinglong Station of National Astronomical Observatories (NAOs) in China, new CCD photometry of TYC 3836-0854-1 was performed from 2017 February 7 to 9. The terminal of the telescope is a high-performance Andor CCD camera and $UBV(RI)_c$ filters were selected for the object. The integration times, related to the filters and weather conditions, were set to 10 to 50 s. A total of 333 points in U band, 330 points in B band, 337 points in V band, 324 points in R_c band, and 334 points in I_c band were obtained. Additionally, complete R_c light curves of TYC 3836-0854-1 was observed with the 50 cm telescope at the Sternberg Astronomical Institute of Russia.

Table 1 lists the coordinates of the variable (V), comparison (C) and check (Ch) stars. The observed images were reduced by using PHOT of the IRAF aperture photometry package. The three groups of phased light curves are plotted in Figure 1, where the differential magnitudes between C and Ch stars are also displayed in the lower part. The light curves of both objects show total eclipses at secondary eclipse (phase = 0.50 P). All observations are tabulated in the form of heliocentric Julian dates (HJD) and the magnitude difference (Δm) between V and C stars and are listed in Table 2. With these observed data and a least squares parabolic fitting method, new times of light minima for both objects were determined and listed in Table 3. In addition, we observed more primary and secondary eclipses with 1.0 m and 60 cm telescopes at YNOs. More new times of light minima were obtained and listed in the Table 3.

[7] http://skydot.lanl.gov/nsvs/nsvs.php

Table 1
Coordinates of the Target, Comparison, and Check Stars

Stars	$\alpha_{2000.0}$	$\delta_{2000.0}$
TYC 1337-1137-1	$06^h35^m46\overset{s}{.}22$	$19°28'28\overset{''}{.}08$
Comparison	$06^h35^m44\overset{s}{.}24$	$19°31'50\overset{''}{.}5$
Check	$06^h35^m26\overset{s}{.}93$	$19°27'26\overset{''}{.}1$
TYC 3836-0854-1	$12^h06^m19\overset{s}{.}797$	$57°10'35\overset{''}{.}21$
TYC 3836-0744-1 (C)	$12^h07^m00\overset{s}{.}482$	$57°11'18\overset{''}{.}49$
TYC 3836-0754-1 (Ch)	$12^h06^m44\overset{s}{.}999$	$57°06'24\overset{''}{.}16$

2.2. Light-curve Analysis and Solutions

We used the W–D 2013 program (Wilson & Devinney 1971; Wilson 1979, 1990, 2012 and Van Hamme & Wilson 2007) to analyze light curves of both objects. Based on the Table 11 given by Ramírez & Meléndez (2005), Gezer & Bozkurt (2016) determined an effective temperature of Star 1 (the star eclipsed at the primary minimum) for TYC 1337-1137-1 as $T_1 = 6229$ K according to the average values of two temperatures calculated with $(V - K_2)$ and $(V_T - K_2)$ colors. Actually, V, K_2, and V_T are magnitudes observed with different photometric systems, sometimes the temperature determined with these color indices will have a significant error. Similarly, Acerbi et al. (2014) estimated the T_1 of TYC 3836-0854-1 to be 6200 K based on the color indices because spectral information was unavailable. During our modeling process, the primary temperatures were taken from the spectral information of the two targets listed in Table 4 released by the Guoshoujing Telescope (the Large Sky Area Multi-Object Fiber Spectroscopic Telescope (LAMOST) (Qian et al. 2017). $T_1 = 6400 \pm 20$ K for the first system and $T_1 = 6332 \pm 52$ K for the second one. The gravity-darkening coefficients $g_{1,2} = 0.32$ (Lucy 1967) and the bolometric albedos $A_{1,2} = 0.5$ (Ruciński 1969) were set for the common convective envelope of both component stars. An internal computation with the logarithmic law was used to obtain the bolometric limb-darkening coefficients and bandpass limb-darkening coefficients.

The mass ratio is a very important parameter. For totally eclipsing over-contact binaries, the mass ratio is well-determined from light curves because of their steep relative radii—surface potential—mass ratio relationship (Terrell & Wilson 2005). A common technique called q-search method was used to obtain initial input values of parameters (i.e., the mass ratio q, the orbital inclination i, the mean temperature of Star 2 T_2, the monochromatic luminosity of Star 1 L_1, and the

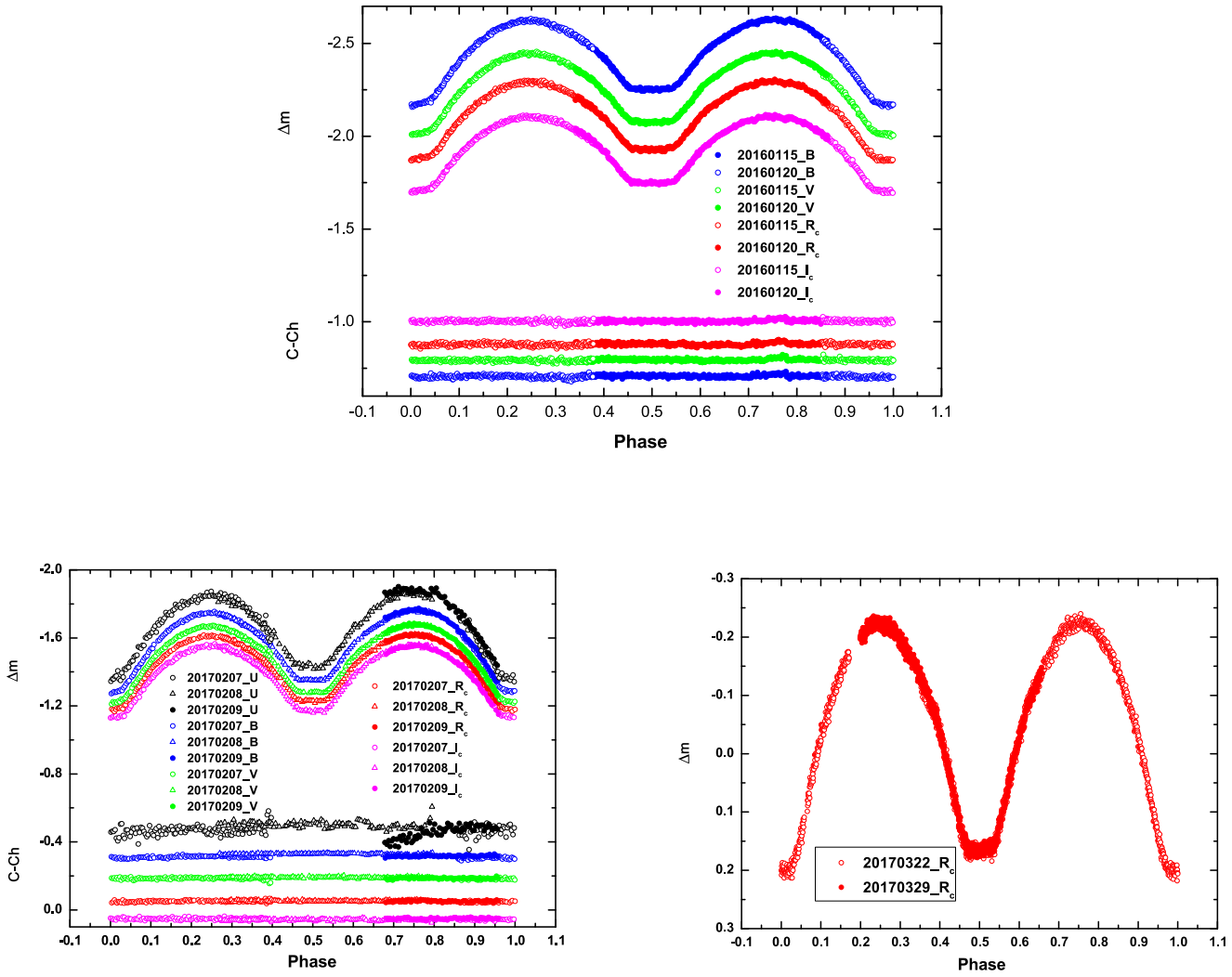

Figure 1. Upper panel: $BV(RI)_c$ light curves of TYC 1337-1137-1 observed using the 1.0 m telescope at YNOs. The differential magnitudes between the comparison (C) and check (Ch) stars are displayed in the lower part. Lower panels: $UBV(RI)_c$ light curves of TYC 3836-0854-1 observed by the 85 cm telescope at the Xinglong Station of NAOs in China, and R_c light curves of TYC 3836-0854-1 observed with the 50 cm telescope at the Sternberg Astronomical Institute of Russia. (A color version of this figure is available in the online journal.)

Table 2
Observations for TYC 1337-1137-1 and TYC 3836-0854-1

TYC 1337-1137-1 (B-Band)							
HJD	Δm	HJD	Δm	HJD	Δm	HJD	Δm
2457403.0274	−2.540	2457403.0320	−2.526	2457403.0366	−2.513	2457403.0412	−2.485
2457403.0282	−2.545	2457403.0328	−2.517	2457403.0374	−2.501	2457403.0420	−2.484
2457403.0290	−2.534	2457403.0335	−2.514	2457403.0381	−2.510	2457403.0427	−2.487
2457403.0297	−2.532	2457403.0343	−2.511	2457403.0389	−2.506	2457403.0435	−2.478
2457403.0305	−2.538	2457403.0351	−2.520	2457403.0397	−2.498	2457403.0442	−2.473
2457403.0313	−2.530	2457403.0358	−2.505	2457403.0404	−2.491	2457403.0450	−2.469

(This table is available in its entirety in machine-readable form in the online version of this article.)

Table 3
New CCD Times of Light Minima for TYC 1337-1137-1 and TYC 3836-0854-1

Date	J. D. (Hel.)	Errors (days)	Min.	Telescope
TYC 1337-1137-1				
2015 Nov 19	2457346.27535	0.00061	p	60 cm
2015 Nov 22	2457349.36601	0.00010	s	60 cm
2016 Jan 15	2457403.10351	0.00008	s	1 m
2016 Jan 20	2457408.09619	0.00021	p	1 m
2017 Jan 14	2457768.06731	0.00013	p	1 m
2017 Feb 16	2457801.11599	0.00006	s	1 m
2017 Feb 17	2457802.06885	0.00002	s	1 m
2017 Mar 04	2457817.04683	0.00004	p	1 m
TYC 3836-0854-1				
2017 Feb 07	2457792.26900	0.00009	p	85 cm
2017 Feb 08	2457793.30759	0.00004	p	85 cm
2017 Mar 22	2457835.48720	0.00007	p	50 cm
2017 Mar 22	2457835.27991	0.00009	s	50 cm
2017 Mar 29	2457842.34462	0.00008	s	50 cm
2017 May 05	2457879.12756	0.00011	p	1 m
2017 May 09	2457883.07483	0.00017	s	60 cm
2017 May 26	2457900.11584	0.00018	s	1m

Note. p refers to the primary minimum and s to the secondary minimum.

Table 4
The Spectral Information of Targets Released by LAMOST

Targets	Obsdate	Subclass	$[F_e/H]$	$T_{\rm eff}$ (K)	$\log(g)$
TYC 1337-1137-1	2012/02/11	F6	0.17 ± 0.01	6400 ± 20	4.07 ± 0.02
TYC 3836-0854-1	2016/01/27	F4	-0.125 ± 0.049	6332.02 ± 51.93	4.030 ± 0.074

dimensionless surface potential $\Omega_1 = \Omega_2$ for contact configuration). During the q-search process, a series of trial values of q were assumed. The resulting sum of the squares of the residuals Σ for each q are plotted in the upper part of Figure 2. It is shown that the minimum values of Σ are achieved at $q = 0.175$, $q = 0.19$, and $q = 0.20$, respectively. The final photometric solutions were obtained and listed in Table 5 by performing a series of differential corrections. Theoretical light curves (color lines) calculated with these solutions are drawn in the lower part of Figure 2. For TYC 3836-0854-1, all the light curves are symmetric but with a small O'Connell effect (O'Connell 1951) in the short wave band observations, which may be caused by the magnetic activities of surface spots. Comparing the solutions for multi-color data (Column 3) and single band data (Column 4), the differences between parameters are very small. This indicates that the photometric solutions are generally stable and reliable. Parameters in Column 3 are recommended for TYC 3836-0854-1 because multi-color solutions are generally considered to be more reliable. The results show that both of them are low-mass ratio, deep overcontact binary systems with a mass ratio of $q = 0.1716 \pm 0.0010$ and a high fillout factor of $f = 76.0 \pm 2.9\%$ for TYC 1337-1137-1, and $q = 0.1900 \pm 0.0032$ and $f = 79.4 \pm 7.9\%$ for TYC 3836-0854-1, respectively. Fillout factor is defined as $f = (\Omega_{\rm in} - \Omega_{\rm star})/(\Omega_{\rm in} - \Omega_{\rm out})$, where $\Omega_{\rm star}$, $\Omega_{\rm in}$ and $\Omega_{\rm out}$ are the modified dimensionless potential of star surface, inner Roche lobe and outer Roche lobe, respectively.

3. The Absolute Parameters

The mass–radius (M–R) relationship was proposed by Zhang et al. (2017) that can be used to calculate the absolute parameters of binaries. The radii relative to the semimajor axis $r_{1,2}$ ($=R_{1,2}/A$) and the mass ratio $q = M_2/M_1$, i.e., $M_{1,2}/M$ were provided by the light-curve analysis, where M and A are the total mass and semimajor axis of a binary system. *Kepler*'s third law can be regarded as a relationship between M and A since the period of two systems is known. Combined with the parameters $M_{1,2}/M$ and $R_{1,2}/A$, the relationships between $M_{1,2}$ and $R_{1,2}$ for the two contact binaries here are obtained:

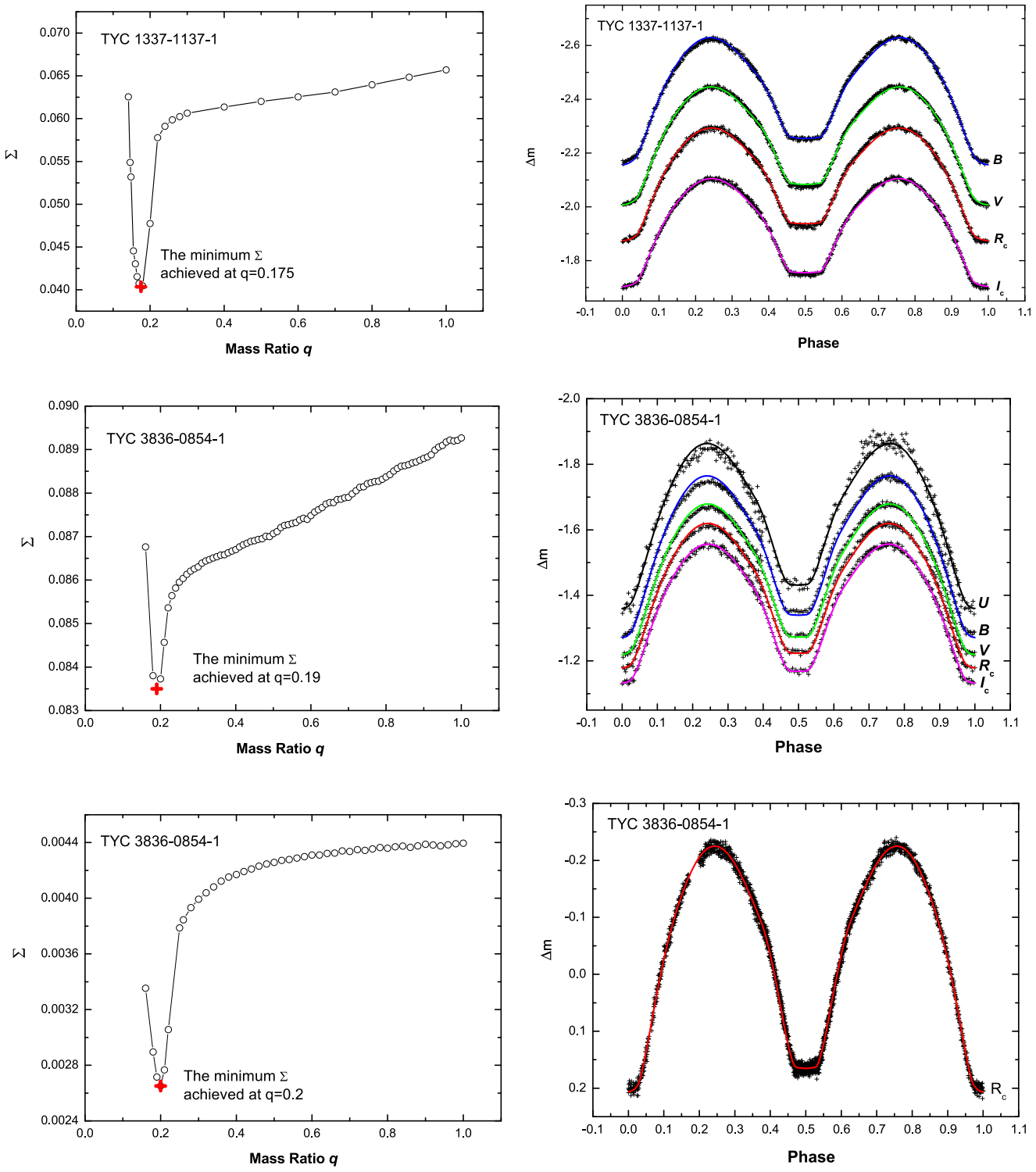

Figure 2. Left panels: the q-search diagrams of TYC 1337-1137-1 and TYC 3836-0854-1. The lowest points (marked in red) locate at $q = 0.175$, $q = 0.19$, and $q = 0.2$, respectively. Right panels: light curves of TYC 1337-1137-1 and TYC 3836-0854-1. The plus signs stand for the observed light curves, while color lines for the theoretical ones. From top to bottom show the light curves observed in 2016 January for TYC 1337-1137-1, 2017 February and March for TYC 3836-0854-1, respectively.

(A color version of this figure is available in the online journal.)

Table 5
Photometric Solutions for TYC 1337-1137-1 and TYC 3836-0854-1

Parameters	TYC 1337-1137-1 (Recommended)	TYC 3836-0854-1 (Data of 85 cm) (Recommended)	TYC 3836-0854-1 (Data of 50 cm)
Mode	Overcontact binary	Overcontact binary	Overcontact binary
Primary temperature T_1[a] (K)	6400	6332	6332
Secondary temperature T_2 (K)	6245(±4)	6292(±10)	6277(±4)
Orbital inclination i(°)	81.03(±0.21)	77.46(±0.40)	78.54(±0.11)
Mass ratio q (M_2/M_1)	0.1716(±0.0010)	0.1900(±0.0032)	0.1989(±0.0007)
Modified dimensionless surface potential ($\Omega_1 = \Omega_2$)	2.0767(±0.0032)	2.1112(±0.0096)	2.1537(±0.0024)
Luminosity ratio $L_{1U}/(L_{1U} + L_{2U})$	…	0.80586(±0.00038)	…
Luminosity ratio $L_{1B}/(L_{1B} + L_{2B})$	0.8343(±0.0001)	0.80415(±0.00040)	…
Luminosity ratio $L_{1V}/(L_{1V} + L_{2V})$	0.8295(±0.0001)	0.80310(±0.00050)	…
Luminosity ratio $L_{1R_c}/(L_{1R_c} + L_{2R_c})$	0.8271(±0.0001)	0.80254(±0.00081)	0.80349(±0.00008)
Luminosity ratio $L_{1I_c}/(L_{1I_c} + L_{2I_c})$	0.8251(±0.0001)	0.80207(±0.00083)	…
Radius of star 1 (relative to semimajor axis) in pole direction r_1(pole)	0.5196(±0.0006)	0.5148(±0.0018)	0.50616(±0.00047)
Radius of star 1 (relative to semimajor axis) in side direction r_1(side)	0.5771(±0.0009)	0.5706(±0.0026)	0.55773(±0.00068)
Radius of star 1 (relative to semimajor axis) in back direction r_1(back)	0.6058(±0.0010)	0.6012(±0.0027)	0.58651(±0.00076)
Radius of star 2 (relative to semimajor axis) in pole direction r_2(pole)	0.2482(±0.0029)	0.2576(±0.0084)	0.2535(±0.0017)
Radius of star 2 (relative to semimajor axis) in side direction r_2(side)	0.2622(±0.0037)	0.273(±0.011)	0.2670(±0.0021)
Radius of star 2 (relative to semimajor axis) in back direction r_2(back)	0.3350(±0.0140)	0.351(±0.043)	0.3263(±0.0059)
Fillout factor f (%)	76.0(±2.9)	79.4(±7.9)	60.1(±1.9)
Equal-volume radius of star 1 (relative to semimajor axis) r_1	0.5678(±0.0005)	0.5628(±0.0014)	0.55065(±0.0037)
Equal-volume radius of star 2 (relative to semimajor axis) r_2	0.2773(±0.0042)	0.288(±0.013)	0.2815(±0.0019)
Radius ratio R_2/R_1	0.4884(±0.0075)	0.512(±0.023)	0.5111(±0.0036)
Theoretical mean density $\rho_1(\rho_\odot)$[b]	0.277(±0.002)	0.367(±0.005)	0.389(±0.001)
Theoretical mean density $\rho_2(\rho_\odot)$[b]	0.408(±0.005)	0.518(±0.017)	0.579(±0.003)

Notes.
[a] The primary temperatures are taken from the spectral data released by LAMOST.
[b] The theoretical mean densities $M\Big/\left(\frac{4}{3}R^3\right)$ in solar unit of 1410.040 842 Kg m^{-3}, which were derived from light-curve analysis (Zhang et al. 2017).

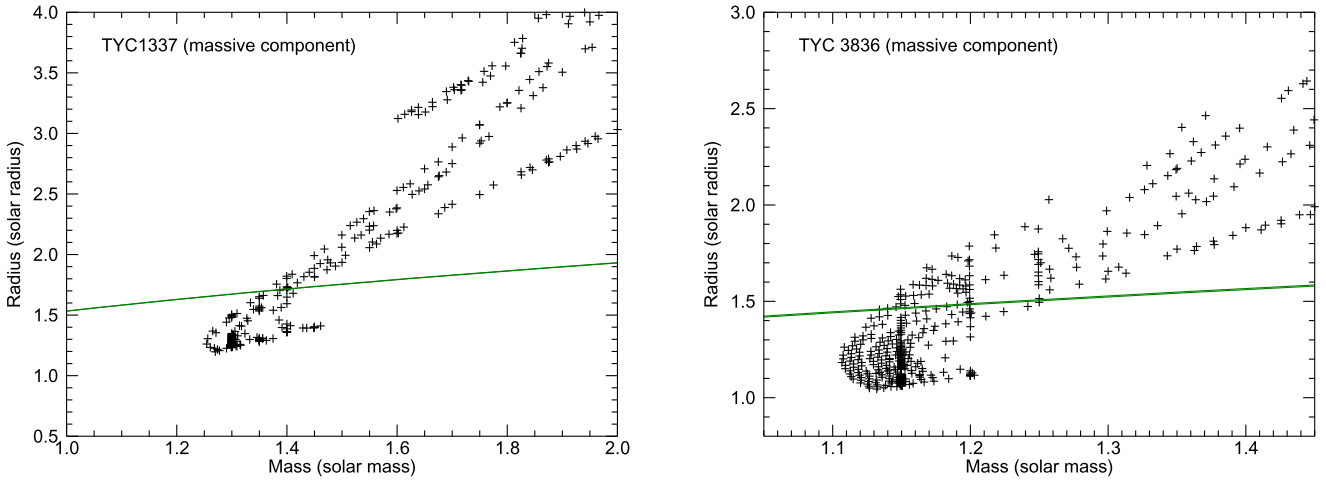

Figure 3. The M–R diagram along with the M–R relationship described by Equation (1) (the belt areas surrounded by the two green lines). The stars generated by the PARSEC program are represented by black plus signs. The temperatures and metallicity range of the black plus are 6380–6420 K and $Z = 0.010$–0.012 for TYC 1337-1137-1, and 6280–6384 K and $Z = 0.02$–0.025 for TYC 3836-0854-1, respectively.
(A color version of this figure is available in the online journal.)

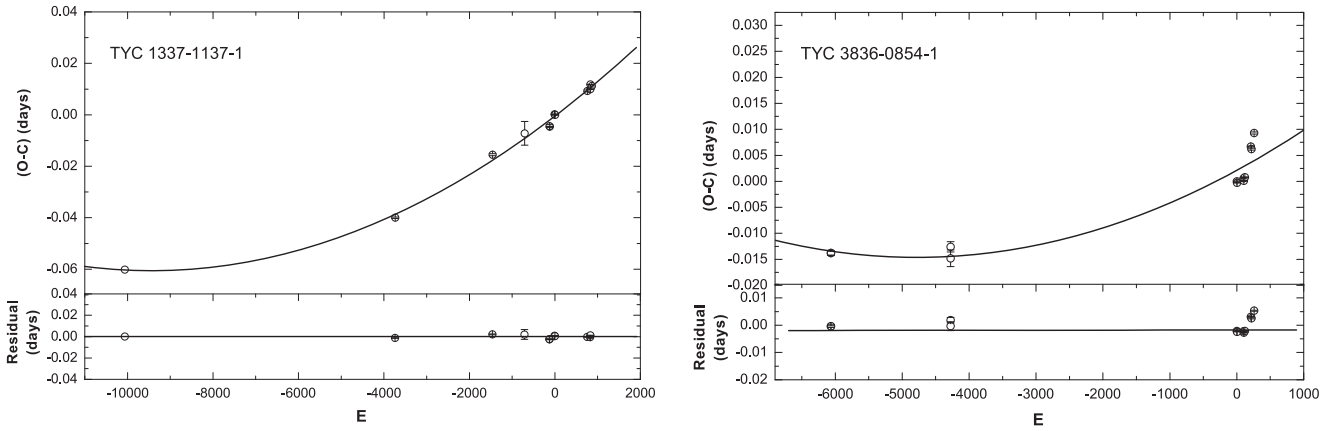

Figure 4. ($O - C$) diagrams of TYC 1337-1137-1 (left) and TYC 3836-0854-1 (right). Long-term period increases are existed for both the systems, which are shown in solid lines in the upper panel. The lower panels are residuals from the whole effect.

Table 6
The Absolute Parameters of TYC 1337-1137-1 and TYC 3836-0854-1

Parameters	TYC 1337-1137-1	TYC 3836-0854-1
$M_1(M_\odot)$	1.386 ± 0.050	1.20 ± 0.07
$M_2(M_\odot)$	0.238 ± 0.009	0.228 ± 0.014
$R_1(R_\odot)$	1.70 ± 0.04	1.46 ± 0.06
$R_2(R_\odot)$	0.83 ± 0.02	0.75 ± 0.05
T_1(K)	6400 ± 20	6332 ± 52
T_2(K)	6245 ± 4	6292 ± 10

the massive component of TYC 1337-1137-1:

$$3.6141(68)\frac{M_1}{M_\odot} = \left(\frac{R_1}{R\odot}\right)^3,$$

the massive component of TYC 3836-0854-1:

$$2.731(15)\frac{M_1}{M_\odot} = \left(\frac{R_1}{R\odot}\right)^3. \quad (1)$$

The evolutionary code PARSEC[8] provides all the star parameters. We selected the stars with a temperature and metallicity range of 6380–6420 K and $Z = 0.010$–0.012 for TYC 1337-1137-1, 6280–6384 K and $Z = 0.02$–0.025 for TYC 3836-0854-1, respectively. These temperature ranges are the massive component's temperature 6400 K with 20 K error (TYC 1337), 6332 K with 52 K error (TYC 3836), and the metallicity range is measured from the spectral data (i.e., $[F_e/H]$ in Table 4). M–R diagrams of TYC 1337-1137-1 (left) and TYC 3836-0854-1 (right) are shown in Figure 3, where the belt areas surrounded by the two green lines are described by Equation (1). Two green lines in each graph are almost coincident, because the errors of parameters derived by the light-curve analysis are very small. The massive components are probably located in the belt area of the black points enclosed by the green lines, and then the absolute parameters are read out from the Figure 3 approximately (Zhang et al. 2017), and listed in Table 6. Comparing to the theoretical mean densities of components presented in Table 5, the mean densities calculated with the masses and radii derived here are in good agreement with them, suggesting that the absolute parameters are correct.

[8] http://stev.oapd.inaf.it/cgi-bin/cmd

4. Orbital Period Changes

Orbital period changes for these two systems have been neglected. By using those new times of light minima listed in the Table 3, four others for TYC 1337-1137-1 (Hubscher et al. 2012; Hubscher 2015; Hubscher & Lehmann 2015; Gezer & Bozkurt 2016) and one for TYC 3836-0854-1 (Acerbi et al. 2014) collected from literatures, the orbital period changes were investigated for the first time. The ($O - C$) values were computed with the following linear ephemeris,
TYC 1337-1137-1:

$$\mathrm{Min}\, I = 2457408.09619 + 0^{\mathrm{d}}.475511 \times E,$$

TYC 3836-0854-1:

$$\mathrm{Min}\, I = 2457792.269 + 0^{\mathrm{d}}.415559 \times E, \quad (2)$$

where HJD_0 is one of the times of light minima obtained in present paper and periods of 0.475511 days (from Gezer & Bozkurt 2016) and 0.415559 days (from Acerbi et al. 2014) were used. The ($O - C$) values versus the epoch number E are displayed in Figure 4. The general ($O - C$) trend of both systems indicate an upward parabolic variation. Then, the following equations are obtained based on the least-squares method:

TYC 1337-1137-1:

$$\mathrm{Min}.I = 2457408.0957265(\pm 0.0000076) + 0.475523770\ (\pm 0.000000027) \times E + 6.779(\pm 0.029) \times 10^{-10} \times E^2,$$

TYC 3836-0854-1:

$$\mathrm{Min}.I = 2457792.2711082(\pm 0.0000152) + 0.415566006\ (\pm 0.000000031) \times E + 6.329(\pm 0.057) \times 10^{-10} \times E^2. \quad (3)$$

The quadratic terms in Equation (3) reveal a long-term period increase at a rate of $dP/dt = +1.04 \times 10^{-6}$ day yr^{-1} for TYC 1337-1137-1 and $dP/dt = +1.11 \times 10^{-6}$ day yr^{-1} for TYC 3836-0854-1, which are displayed in solid lines in the upper panels of Figure 4. The residuals are plotted in the lower panels of the Figure 4, where no variations can be traced.

5. Discussions and Conclusions

The photometric solutions for TYC 1337-1137-1 and TYC 3836-0854-1 were derived based on multi-color light curves. It is shown that both of them are low-mass ratio, deep overcontact binary systems with a mass ratio of $q = 0.1716 \pm 0.0010$ and a high fillout factor of $f = 76.0 \pm 2.9\%$ for TYC 1337-1137-1, and $q = 0.1900 \pm 0.0032$ and $f = 79.4 \pm 7.9\%$ for TYC 3836-0854-1, respectively. The degree of contact factors for both systems determined in present paper are larger than the values given by previous authors. The present solutions may be more plausible and reliable, because (1) the spectral information are available here and (2) for TYC 1337-1137-1, our good quality light curves are observed in multi-color and analyzed simultaneously; for TYC 3836-0854-1, photometric solutions of two sets of observations have small differences between most parameters.

By using the *M–R* relationship from the light-curve analysis and spectral data given by LAMOST, the absolute parameters are re-estimated: $M_1 = 1.386 \pm 0.050\ M_\odot$, $M_2 = 0.238 \pm 0.009\ M_\odot$, $R_1 = 1.70 \pm 0.04$, and $R_2 = 0.83 \pm 0.02$ for TYC 1337-1137-1. $M_1 = 1.20 \pm 0.07\ M_\odot$, $M_2 = 0.228 \pm 0.014\ M_\odot$, $R_1 = 1.46 \pm 0.06$, and $R_2 = 0.75 \pm 0.05$ for TYC 3836-0854-1.

The preliminary changes in orbital period were also discussed by using all available times of light minima. Although the time span of the data is not long, the current data have already reflected a variation of an upward parabolic at a rate of $dP/dt = +1.04 \times 10^{-6}$ day yr^{-1} for TYC 1337-1137-1 and $+1.11 \times 10^{-6}$ day yr^{-1} for TYC 3836-0854-1, respectively. The long-term period increase of such system may be interpreted in two possible ways. A first possibility is mass transfer conservation from the less massive component to the more massive one leading to an orbital period increase. In this case, when their orbital angular momentum is less than three times the total spin angular momentum, i.e., $J_{\rm orb} < 3\ J_{\rm spin}$, TYC 1337-1137-1 and TYC 3836-0854-1 may evolve from their current deep overcontact state into a rapidly rotating single star (Hut 1980). A second possibility is that the parabolic variation in the $(O - C)$ diagram is only a part of a long-period cyclic change caused by a potential third body (Liao & Qian 2010; Chambliss 1992). In the future, the form of orbital period change needs to be confirmed by more observations.

This work is supported by the National Natural Science Foundation of China (Nos. 11403095, 11325315, and 11611530685) and the Yunnan Natural Science Foundation (2014FB187). New CCD observations were obtained with the 1 m and 60 cm telescopes at Yunnan Observatories, the 85 cm telescope at Xinglong station, National Astronomical Observatories and 50 cm telescope in Sternberg Astronomical Institute of Russia. The spectral data were provided by Guoshoujing Telescope (the Large Sky Area Multi-Object Fiber Spectroscopic Telescope, (LAMOST), which is a National Major Scientific Project built by the Chinese Academy of Sciences. Funding for the project has been provided by the National Development and Reform Commission. LAMOST is operated and managed by the National Astronomical Observatories, Chinese Academy of Sciences.

References

Acerbi, F., Barani, C., & Martignoni, M. 2014, NewA, 31, 1
Chambliss, C. R. 1992, in Proc. IAU Symp. 151, Evolutionary Processes in Interacting Binary Stars, ed. Y. Kondo, R. F. Sistero, & R. S. Polidan (Dordrecht: Kluwer), 315
Cox, A. N. 2000, Allen's Astrophysical Quantities (4th ed.; New York: Springer)
Gettel, S. J., Geske, M. T., & McKay, T. A. 2006, AJ, 131, 621
Gezer, İ., & Bozkurt, Z. 2016, NewA, 44, 40
Hubscher, J. 2015, IBVS, 6152
Hubscher, J., & Lehmann, P.-B. 2015, IBVS, 6149
Hubscher, J., Lehmann, P.-B., & Walter, F. 2012, IBVS, 6010
Hut, P. 1980, A&A, 92, 167
Liao, W.-P., & Qian, S.-B. 2010, MNRAS, 405, 1930
Lucy, L. B. 1967, ZAp, 65, 89
O'Connell, D. J. K. 1951, PRCO, 2, 85
Paczyński, B., Szczygieł, D. M., Pilecki, B., & Pojmański, G. 2006, MNRAS, 368, 1311
Prša, A., & Zwitter, T. 2005, ApJ, 628, 426
Qian, S.-B., He, J.-J., Zhang, J., et al. 2017, RAA, 17, 87
Qian, S.-B., Liu, L., Soonthornthum, B., Zhu, L.-Y., & He, J.-J. 2006, AJ, 131, 3028
Qian, S.-B., Liu, L., Soonthornthum, B., Zhu, L.-Y., & He, J.-J. 2007, AJ, 134, 1475
Qian, S.-B., Liu, L., Zhu, L.-Y., et al. 2011, AJ, 141, 151
Qian, S.-B., Yang, Y.-G., Soonthornthum, B., et al. 2005a, AJ, 130, 224
Qian, S.-B., Zhu, L.-Y., Soonthornthum, B., et al. 2005b, AJ, 130, 1206
Ramírez, I., & Meléndez, J. 2005, ApJ, 626, 465
Ruciński, S. M. 1969, AcA, 19, 245
Sriram, K., Malu, S., Choi, C. S., & Vivekananda Rao, P. 2016, AJ, 151, 69
Terrell, D., & Wilson, R. E. 2005, Ap&SS, 296, 221
Tylenda, R., Hajduk, M., Kamiński, T., et al. 2011, A&A, 528, 114
Van Hamme, W., & Wilson, R. E. 2007, ApJ, 661, 1129
Wilson, R. E. 1979, ApJ, 234, 1054
Wilson, R. E. 1990, ApJ, 356, 613
Wilson, R. E. 2012, AJ, 144, 73
Wilson, R. E., & Devinney, E. J. 1971, ApJ, 166, 605
Zhang, J., Qian, S.-B., Han, Z.-T., & Wu, Y. 2017, MNRAS, 466, 1118
Zhu, L.-Y., Zhao, E.-G., & Zhou, X. 2016, RAA, 16, 68